J. Plasma Physics (2007), *vol.* 73, *part* 5, *pp.* 701–713. © 2006 Cambridge University Press
doi:10.1017/S002237780600612X First published online 23 October 2006 Printed in the United Kingdom

Wave dynamics of an electrojet: generalized Farley–Buneman instability

JAMES F. McKENZIE[1,2]

[1]Department of Physics, IGPP, University of California, Riverside, CA, 92521 USA
[2]School of Pure and Applied Physics and the Astrophysics and Cosmology Research Unit, School of Mathematical Sciences, University of KwaZulu-Natal, Durban 4001, South Africa

(Received 9 May 2006, revised 18 July 2006, accepted 19 July 2006)

Abstract. In this paper we generalize the classical Farley–Buneman (FB) instability to include space-charge effects and finite electron inertia. The former effect makes the ion-acoustic wave dispersive with the usual resonance appearing at the ion plasma frequency, but other than that the structure of the FB instability remains intact. However, the inclusion of the latter, finite electron inertia, gives rise to the propagating electron-cyclotron mode, albeit modified by collisions. In the presence of differential electron streaming relative to the ions, the interaction between this mode, attempting to propagate against the stream, but convected forward by the stream, and a forward propagating ion-acoustic mode, gives rise to a new instability distinct from the FB instability. The process may be thought of in terms of the coupling between negative energy waves (electron-cyclotron waves attempting to propagate against the stream) and positive energy waves (forward propagating ion-acoustic waves). In principle, the instability simply requires super-ion acoustic streaming electrons and the corresponding growth rates are of the order of one half of the lower hybrid frequency, which are faster than the corresponding FB growth rates. For conditions appropriate to the middle day-side E-region this instability excites a narrow band of frequencies just below the ion plasma frequency. Its role in the generation of electrojet irregularities may be as important as the classical FB instability.

1. Introduction

The Farley–Buneman (FB) instability arises in the lower E-region of the ionosphere where a substantial $\mathbf{E} \times \mathbf{B}/B^2$ drift of the electrons relative to the (essentially un-magnetized) ions (mainly oxygen) can generate unstable ion-acoustic waves. The original formulation was based on treating the electrons as being inertialess and the wave perturbations as quasi-charge neutral, although this has been extended to include the effects of magnetized ions by Fejer et al. (1984).

There has been a considerable amount of work done on the role of this instability and its nonlinear phase, on irregularities in the electrojet (e.g. Weinstock and Sleeper 1972; Sudan 1983; Hamza and St-Maurice 1993; Robinson 1994, 1998; Janhunen 1995; Oppenheim et al. 1996; Liperovsky et al. 1999; Milikh and Diment 2003). In this paper we point out that if electron inertia is included another instability may be generated under similar threshold conditions to the original FB instability. This instability comes about from an interaction between a negative energy electron-cyclotron mode (ECM) and a positive energy ion-acoustic wave in the presence of

https://doi.org/10.1017/S002237780600612X Published online by Cambridge University Press

'supersonic' differential streaming between the electrons and ions. The growth rate of this new instability is of the order of one half of the lower hybrid frequency. In the next section we develop the governing equations for the plasma in the presence of crossed electric and magnetic fields, including collisions with neutrals. Linearization of the equations around the background state yields the dispersion equation for the system. In the case of un-magnetized ions, inertialess electrons and quasi-charge neutrality, this dispersion relation yields the threshold conditions and growth rate for the classical FB instability, namely that the electrons must stream at super-ion acoustic speeds, perpendicular to the background crossed electric and magnetic fields. In this approximation, the ECM, although collision dominated and evanescent, provides the catalyst for the ion-acoustic mode to be driven unstable by the streaming electrons. For wave perturbations propagating along the electron stream (and therefore perpendicular to the magnetic field $\mathbf{B}$) the growth rate has an upper limit of the order of 10^4 s^{-1}, as discussed in Sec. 3. In Sec. 4 we analyze a new instability which hinges on properties of the ECM in the presence of streaming. In a rest frame the wave normal surface of this mode is simply a cone of opening angle $\cos^{-1}(\omega/\Omega_e)$ about $\mathbf{B}_0$. However, in a frame relative to which the electrons stream, the Doppler shifting of the wave frequency means that the cone becomes squashed between two planes representing where the Doppler shifted wave frequency $\omega_e = \omega - \mathbf{k}\cdot\mathbf{U}_e$ matches the electron gyrofrequency (see below and Fig. 1). A branch of this distorted wave normal surface corresponds to waves attempting to propagate against the stream, but are in fact 'blown' in the direction of the stream. Since these waves now possess a negative Doppler shifted frequency $\omega - \mathbf{k}\cdot\mathbf{U}_e$ they may be deemed to carry negative energy. The interaction between these negative energy electron-cyclotron waves and the positive energy ion-acoustic modes (see Fig. 2) gives rise to an instability. The growth rate is of the order of $\sqrt{\Omega_e\Omega_i}/2$, modified somewhat by collisions, and is therefore faster than the classical FB instability. In the lower E-region, the threshold conditions, imposed by collisions with neutrals, are unlikely to be met except for exceptionally strong electric fields. However, in the middle day-side E-region, where the collision frequencies have decreased by an order of magnitude, the threshold conditions are met, and a narrow band of frequencies near the ion plasma frequency are excited over almost all angles except those parallel and perpendicular to the magnetic field.

2. Governing equation

2.1. Background plasma

We consider a simple model of a background plasma in the presence of crossed electric ($E_0\hat{\mathbf{y}}$) and magnetic ($B_0\hat{\mathbf{z}}$) fields in which electrons (e) and ions (i) undergo drifting motions $\mathbf{U}_e$ and $\mathbf{U}_i$ whilst colliding with neutrals (n) with collision frequencies ν_{en} and ν_{in}. In the case where the auroral electrojet $\mathbf{B}_0$ is vertical, $\mathbf{E}_0$ is East–West (zonal), whereas in the equatorial case $\mathbf{B}_0$ is horizontal (North–South) and $\mathbf{E}_0$ (secondary field) is vertical. Assuming that the flows are steady ($\partial/\partial t = 0$) and uniform ($\nabla = 0$) the motion is given by

$$\frac{e}{m_e}(\mathbf{E}_0 + \mathbf{U}_e \times \mathbf{B}_0) = -\nu_{en}\mathbf{U}_e, \tag{2.1a}$$

$$\frac{e}{m_i}\mathbf{E}_0 = \nu_{in}\mathbf{U}_i, \tag{2.1b}$$

https://doi.org/10.1017/S002237780600612X Published online by Cambridge University Press

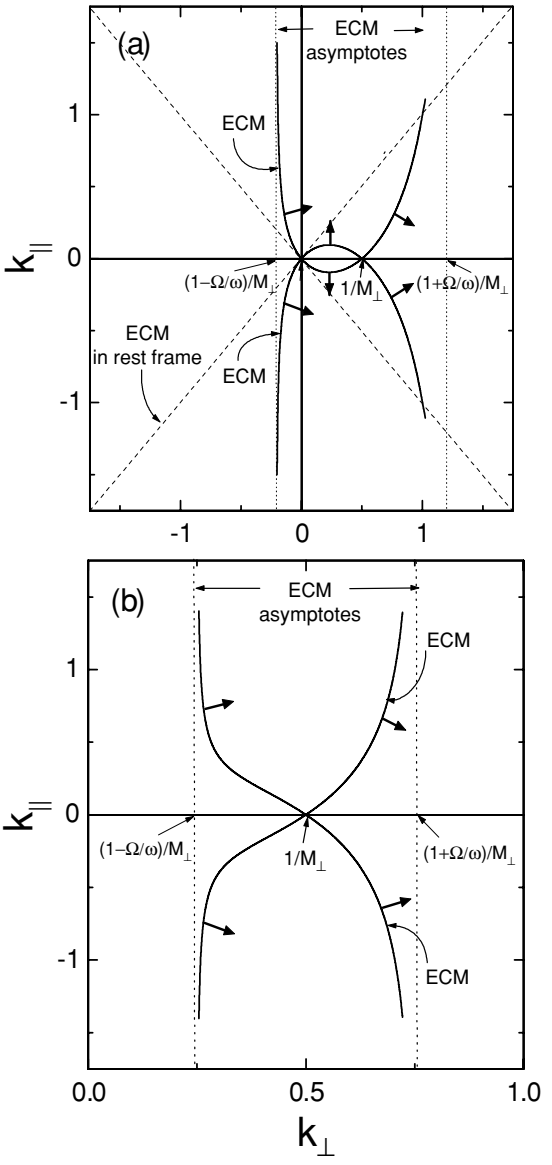


Figure 1. Wave normal curves for the ECM in the presence of electron streaming characterized by $M_\perp = 2$: (a) for $\varpi(=\omega/\Omega) = 1/\sqrt{2}$ (i.e. < 1), and (b) for $\varpi = \sqrt{2}$ (i.e. > 1). In the branches lying in the range $1/M_\perp < k_\perp < (1 + 1/\varpi)1/M_\perp$ the Doppler-shifted wave frequency ω_e is negative.

in which we have assumed the ions to be unmagnetized, which is a good approximation if $\nu_{in} \gg \Omega_i = eB_0/m_i$. Although the gravitational force plays an important role in the Rayleigh–Taylor instability in the ionosphere it may be neglected in the FB instability since its acceleration (g = 10 m s^{-2}) is very much smaller than a typical electric acceleration (eE_0/m_i), which is of the order of 3×10^3 m s^{-2} for $E_0 = 1$ mV m^{-1}. Therefore, the crossed electric and magnetic fields give rise to

https://doi.org/10.1017/S002237780600612X Published online by Cambridge University Press

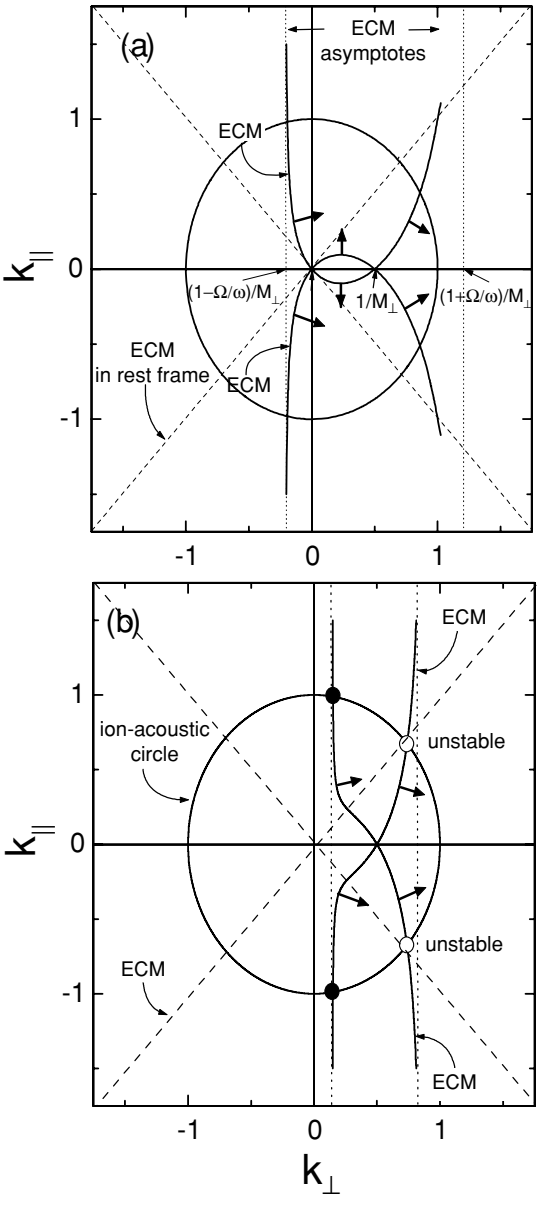


Figure 2. Geometric interpretation of the instability condition plotted for $M_\perp = 2$: (a) for $\overline{\omega} = 1/\sqrt{2}$, and (b) $\overline{\omega} = \sqrt{2}$. The wave normal curve for the ECM is a cone distorted by Doppler shifting arising from electron streaming along the x-axis, and is squashed between the two asymptotes representing wave frequencies, in the rest frame, matching the electron gyrofrequency. In the neighborhood of the intersections between the ECM curves and the acoustic circle, instabilities arise at the points marked O (see Sec. 4). In the ECM branch lying between $1/M_\perp < k_\perp < (1+1/\overline{\omega})/M_\perp$ the wave frequency is negative in the rest frame and this mode may be called a negative energy wave. Alternatively, it may be viewed as the ECM mode propagating against the stream U_{ex}, but is convected forward by the streaming, so as to couple with a forward-propagating ion-acoustic mode.

https://doi.org/10.1017/S002237780600612X Published online by Cambridge University Press

drifting motions

$$\mathbf{U}_\mathrm{e} = \frac{eE_0}{m_\mathrm{e}}\left(\frac{1}{\Omega_\mathrm{e}^2+\nu_\mathrm{en}^2}\right)(\Omega_\mathrm{e}, -\nu_\mathrm{en}, 0) \tag{2.2a}$$

$$= \frac{U_0}{(1+\nu_\mathrm{en}^2/\Omega_\mathrm{e}^2)}(1, -\nu_\mathrm{en}/\Omega_\mathrm{e}, 0), \tag{2.2b}$$

and

$$\mathbf{U}_\mathrm{i} = \frac{eE_0}{m_\mathrm{i}\nu_\mathrm{in}}(0, 1, 0), \tag{2.2c}$$

where U_0 is the E_0/B_0 convection speed and $\Omega_\mathrm{e} = eB_0/m_\mathrm{e}$ is the electron gyrofrequency. It follows that the power expended by $\mathbf{J}_0 \cdot \mathbf{E}_0$, given by

$$\mathbf{J}_0 \cdot \mathbf{E}_0 = eN_0(U_{\mathrm{i}y} - U_{ey})E_0 = e^2N_0E_0^2\left[\frac{1}{m_\mathrm{i}\nu_\mathrm{in}} + \frac{\nu_\mathrm{en}}{m_\mathrm{e}(\Omega_\mathrm{e}^2+\nu_\mathrm{en}^2)}\right], \tag{2.3a}$$

is exactly balanced by the rate of working of the collisional forces,

$$m_\mathrm{i}\nu_\mathrm{in}N_0U_\mathrm{iy}^2 + m_\mathrm{e}\nu_\mathrm{en}N_0U_\mathrm{e}^2, \tag{2.3b}$$

on using (2.2) for the ion and electron velocities, in which N_0 is the background electron and ion number density.

2.2. Linearized perturbations about the background: dispersion equation for the system

We follow the formulation presented in a recent paper by Buchert et al. (2006), but include electron inertia and relax the quasi-charge neutral approximation.

The perturbed system is governed by mass and momentum conservation that, on linearization, may, in obvious notation, be written as

$$\frac{D_\alpha}{Dt}(n_\alpha) = -N_0\nabla\cdot\mathbf{u}_\alpha, \quad \alpha = \mathrm{i}, \mathrm{e}, \tag{2.4}$$

$$m_\mathrm{i}\frac{D_\mathrm{i}}{Dt}(\mathbf{u}_\mathrm{i}) = e\mathbf{E} - \frac{1}{N_0}\nabla p_\mathrm{i} - m_\mathrm{i}\nu_\mathrm{in}\mathbf{u}_\mathrm{i}, \tag{2.5}$$

$$m_\mathrm{e}\frac{D_\mathrm{e}}{Dt}(\mathbf{u}_\mathrm{e}) = -e(\mathbf{E} + \mathbf{u}_\mathrm{e}\times\mathbf{B}_0) - \frac{1}{N_0}\nabla p_\mathrm{e} - m_\mathrm{e}\nu_\mathrm{en}\mathbf{u}_\mathrm{e}, \tag{2.6}$$

$$\frac{D_\alpha}{Dt} \equiv \frac{\partial}{\partial t} + \mathbf{U}_\alpha\cdot\nabla, \tag{2.7}$$

in which we have again assumed that the ions are unmagnetized, which is valid for time scales shorter than an ion gyroperiod. The perturbed electric field $\mathbf{E}$ is given, in this electrostatic treatment, by Poisson's equation

$$\nabla\cdot\mathbf{E} = \frac{e}{\varepsilon_0}(n_\mathrm{i} - n_\mathrm{e}). \tag{2.8}$$

We shall also assume that the pressure p_α and density perturbations are related through an adiabatic law

$$p_\alpha = \gamma_\alpha kT_\alpha n_\alpha, \tag{2.9}$$

where T_α is the background species temperature. In the presence of collisions with neutrals, adiabatic flow is not strictly true, but it does serve as a reasonable approximation. By taking the divergence of the ion equation of motion (2.5) and

https://doi.org/10.1017/S002237780600612X Published online by Cambridge University Press

using ion continuity ((2.4) with $\alpha = \mathrm{i}$), (2.9), and Poisson's equation we obtain

$$\left[\left(\frac{D_\mathrm{i}}{Dt} + \nu_\mathrm{i}\right)\frac{D_\mathrm{i}}{D_t} - c_\mathrm{i}^2\nabla^2 + \omega_\mathrm{pi}^2\right]n_\mathrm{i} = \omega_\mathrm{pi}^2 n_\mathrm{e}, \tag{2.10}$$

in which c_i and ω_pi are, respectively, the ion sound speed and plasma frequency,

$$c_\mathrm{i}^2 = \frac{\gamma_\mathrm{i} k T_\mathrm{i}}{m_\mathrm{i}}, \quad \omega_\mathrm{pi}^2 = \frac{e^2 N_0}{\varepsilon_0 m_\mathrm{i}}. \tag{2.11}$$

The Fourier image of (2.10) for waves proportional to $\exp i(\omega t - \mathbf{k}\cdot\mathbf{r})$ may be written as

$$n_\mathrm{i} = \frac{n_\mathrm{e}}{(1 - d_\mathrm{i})}, \tag{2.12a}$$

in which

$$d_\mathrm{i} \equiv \frac{\omega_\mathrm{i}(\omega_\mathrm{i} - i\nu_\mathrm{in}) - c_\mathrm{i}^2 k^2}{\omega_\mathrm{pi}^2}, \tag{2.12b}$$

$$\omega_\mathrm{i} \equiv \omega - \mathbf{k}\cdot\mathbf{U}_\mathrm{i} = \omega - k_y U_{\mathrm{i}y}. \tag{2.12c}$$

For economy of notation we have simply replaced $n_\alpha(x,t) \to n_\alpha(\omega,\mathbf{k}) \to n_\alpha$. Here ω_i is the wave frequency, Doppler shifted by the background drifting ion motion. Similarly, by adding the ion and electron equations of motion and taking its Fourier image, we have

$$m_\mathrm{e}(\omega_\mathrm{e} - i\nu_\mathrm{en})\mathbf{u}_\mathrm{e} + m_\mathrm{i}(\omega_\mathrm{i} - i\nu_\mathrm{in})\mathbf{u}_\mathrm{i} = \mathbf{k}\left(m_\mathrm{i}c_\mathrm{i}^2\frac{n_\mathrm{i}}{N_0} + m_\mathrm{e}c_\mathrm{e}^2\frac{n_\mathrm{e}}{N_0}\right) + m_\mathrm{e}\Omega_\mathrm{e}\mathbf{u}_\mathrm{e} \tag{2.13}$$

where ω_e is the wave frequency, Doppler shifted by the background streaming electrons, $\omega_\mathrm{e} = \omega - \mathbf{k}\cdot\mathbf{U}_\mathrm{e}$ and $c_\mathrm{e}^2 = \gamma_\mathrm{e} k T_c/m_\mathrm{e}$ is the square of the electron sound speed.

In this, the electrostatic case, we have

$$\mathbf{E} = -\nabla\phi = i\mathbf{k}\phi. \tag{2.14}$$

The Fourier image of the ion equation of motion shows that the perturbed ion velocity $\mathbf{u}_\mathrm{i}$ is parallel to the wave number vector $\mathbf{k}$, and ion continuity therefore requires

$$\mathbf{u}_\mathrm{i} = \omega_\mathrm{i}\frac{n_\mathrm{i}}{N_0}\frac{\mathbf{k}}{k^2} \tag{2.15a}$$

$$= \omega_\mathrm{i}\frac{n_\mathrm{e}}{N_0(1 - d_\mathrm{i})}\frac{\mathbf{k}}{k^2}, \tag{2.15b}$$

the latter following on using (2.12a). Eliminating $\mathbf{u}_\mathrm{i}$ and n_i from (2.13) yields

$$(\omega_\mathrm{e} - i\nu_\mathrm{en}\mathbf{u}_\mathrm{e}) - i\Omega_\mathrm{e}\mathbf{u}_\mathrm{e} = \frac{n_\mathrm{e}}{N_0}R\mathbf{k} \tag{2.16a}$$

with

$$R \equiv \frac{m_\mathrm{i}}{m_\mathrm{e}}\left[c_\mathrm{ei}^2 - \frac{\omega_\mathrm{pi}^2}{k^2}\frac{d_\mathrm{i}}{(1 - d_\mathrm{i})}\right]. \tag{2.16b}$$

Equation (2.16a) may be expressed in explicit component form

$$\mathbf{u}_\mathrm{e} = (u_{ex}, u_{ey}, u_{ez}) = \frac{n_\mathrm{e}}{N_0}\mathbf{C}, \tag{2.17a}$$

https://doi.org/10.1017/S002237780600612X Published online by Cambridge University Press

with

$$\mathbf{C} \equiv R\left[\frac{(\omega_e - i\nu_{en})k_x + ik_y\Omega_e}{(\omega_e - i\nu_{en})^2 - \Omega_e^2}, \frac{(\omega_e - i\nu_{en})k_y - ik_x\Omega_e}{(\omega_e - i\nu_{en})^2 - \Omega_e^2}, \frac{k_z}{(\omega_e - i\nu_{en})}\right]. \tag{2.17b}$$

Therefore, on taking the scalar product of (2.17a) with $\mathbf{k}$ and eliminating $\mathbf{u}_e$, using electron continuity,

$$\mathbf{k}\cdot\mathbf{u}_e = \omega_e\frac{n_e}{N_0}, \tag{2.18}$$

we obtain the dispersion equation for the perturbed system,

$$\omega_e = \mathbf{k}\cdot\mathbf{C} \tag{2.19a}$$

$$= R\left[\frac{(\omega_e - i\nu_{en})k_\perp^2}{(\omega_e - i\nu_{en})^2 - \Omega_e^2} + \frac{k_\parallel^2}{(\omega_e - i\nu_{en})}\right], \tag{2.19b}$$

or alternatively

$$\frac{m_e}{m_i} = \left[c_{ei}^2k^2 - \frac{\omega_{pi}^2 d_i}{(1-d_i)}\right]\left[\frac{(\omega_e - i\nu_{en})\sin^2\theta/\omega_e}{(\omega_e - i\nu_{en})^2 - \Omega_e^2} + \frac{\cos^2\theta/\omega_e}{(\omega_e - i\nu_{en})}\right], \tag{2.19c}$$

in which $c_{ei} = \sqrt{k\gamma_e T_e/m_i}$ is the ion-acoustic speed, $k_\perp = \sqrt{k_x^2 + k_y^2}$, $k_\parallel = k_z$ and θ is the angle between $\mathbf{k}$ and $\mathbf{B}_0$. Equations (2.19a–c) represent a generalization of the original FB dispersion equation to include electron inertia and space charge effects (through Poisson's equation, which implies that $n_i \neq n_e$) as measured by the quantity d_i (see (2.12b)).

There are three modes embedded in (2.19). In the collisionless case ($\nu_i = \nu_e = 0$) and $m_e/m_i \to 0$, the zero of the first bracket on the right-hand side of (2.19c) is the ion-acoustic mode, which, in the cold ion case, gives

$$c_{ei}^2k^2 = \frac{\omega_i^2}{(1 - \omega_i^2/\omega_{pi}^2)}, \tag{2.20}$$

whilst the zero of the second bracket describes the ECM

$$\omega_e = \pm\Omega_e\cos\theta, \tag{2.21a}$$

or

$$\frac{k_\perp^2}{k_\parallel^2} = \left(\frac{\Omega_e^2}{\omega_e^2} - 1\right). \tag{2.21b}$$

Equation (2.20) describes ion-acoustic waves exhibiting a resonance at the ion-plasma frequency. The wave normal diagram for the ECM, in the rest frame of the electrons, is a cone of opening angle $\cos^{-1}(\omega_e/\Omega_e)$ and, therefore, only propagates for $\omega_e < \Omega_e$. The high-frequency Langmuir wave emerges from (2.19) by using the limits $d_i \to \infty$, $\omega_e \gg \Omega_e$ and ν_{en}, to give

$$\frac{m_e}{m_i} = (c_{ei}^2k^2 + \omega_{pi}^2)\frac{1}{\omega_e^2}, \tag{2.22a}$$

which rearranges to the classical Langmuir wave

$$\omega_e^2 = c_e^2k^2 + \omega_{pe}^2. \tag{2.22b}$$

Before analyzing the possible instabilities described by the general dispersion relation we note that, in a laboratory frame relative to which the electrons are

https://doi.org/10.1017/S002237780600612X Published online by Cambridge University Press

streaming, the cone, given by (2.21), becomes distorted by the Doppler shift, $\omega_e = \omega - \mathbf{k}_\perp \cdot \mathbf{U}_{\perp e}$, with the result

$$k_\parallel^2 = \frac{k_\perp^2(\omega - \mathbf{k}_\perp \cdot \mathbf{U}_{\perp e})^2}{[\Omega_e^2 - (\omega - \mathbf{k}_\perp \cdot \mathbf{U}_{\perp e})^2]} \tag{2.23a}$$

or, in the case $\mathbf{k} = (k_x, 0, k_z)$,

$$k_z^2 = \frac{k_x^2(\omega - k_x U_0)^2}{[\Omega_e^2 - (\omega - k_x U_0)^2]} \tag{2.23b}$$

from which we see a cut-off

$$k_z = 0 \tag{2.24}$$

at $k_x = \omega/U_0$, and a resonance

$$k_z = \infty \tag{2.25}$$

at $k_x = (\omega \pm \Omega_e)/\Omega_e$.

The distorted wave normal curve, shown in Fig. 1(a), is a cone squashed between the two planes $\omega_e = \pm\Omega_e$. The small arrows drawn normal to the wave normal curve indicate the ray direction. As we shall see subsequently, the interactions between this distorted electron-cyclotron cone and the ion-acoustic sphere can give rise to unstable interactions. It is also worth noting that the wave propagates for $(\omega > \Omega_e)$, as shown in Fig. 1(b), as a result of the Doppler shift, which in these regions of $\mathbf{k}$-space makes the frequency $\omega_e < \Omega_e$.

3. The low-frequency instability: the Farley–Buneman case

If we impose charge neutrality, $d_i \to 0, \omega_i \ll \omega_{pi}$, and neglect electron inertia, $\omega_e \ll \nu_e$, the dispersion relation (2.19) simplifies somewhat to

$$\omega_e \equiv \omega - \mathbf{k} \cdot \mathbf{U}_e = \frac{m_i}{m_e} \frac{(\nu_e^2 + \Omega_e^2 \cos^2\theta)}{\nu_e(\nu_e^2 + \Omega_e^2)} [-i(\omega^2 - c_{ei}^2 k^2) - \omega\nu_i], \tag{3.1}$$

in which we have also neglected the much smaller ion streaming, $\omega_i \to \omega$, compared with the electron steaming. Splitting ω into its real and imaginary parts, i.e. $\omega = \omega_r - i\gamma$, and equating real and imaginary parts of (3.1) we obtain

$$\omega_r - \mathbf{k} \cdot \mathbf{U}_e = \frac{m_i}{m_e} \frac{(\nu_e^2 + \Omega_e^2 \cos^2\theta)}{\nu_e(\nu_e^2 + \Omega_e^2)} (-\nu_i\omega_r - 2\omega_r\gamma) \tag{3.2a}$$

and

$$-\gamma = \frac{m_i}{m_e} [\nu_i\gamma - (\omega_r^2 - \gamma^2 - c_{ei}^2 k^2)]. \tag{3.2b}$$

In (3.2a), if we assume that the growth rate $\gamma\ (>0) \ll \nu_i$, the real frequency may be written as

$$\omega_r = \frac{\mathbf{k} \cdot \mathbf{U}_e}{1 + \psi}, \tag{3.3a}$$

where

$$\psi \equiv \frac{m_i}{m_e} \frac{(\nu_e^2 + \Omega_e^2 \cos^2\theta)\nu_i}{\nu_e(\nu_e^2 + \Omega_e^2)}, \tag{3.3b}$$

whereas the growth rate γ is now given by

$$\gamma = \frac{\psi}{\nu_i} \frac{(\omega_r^2 - c_{ei}^2 k^2)}{1 + \psi}. \tag{3.3c}$$

https://doi.org/10.1017/S002237780600612X Published online by Cambridge University Press

Hence we have instability, $\gamma > 0$, provided $\omega_r^2 > c_{ei}^2 k^2$, which, on using (3.3a), translates into the condition

$$(\mathbf{k} \cdot \mathbf{U}_e)^2 > c_{ei}^2 k^2 (1 + \psi)^2. \tag{3.4}$$

Thus electrons streaming 'super ion-acoustically' generate a cone of unstable waves about the direction of streaming. In this process, the highly collisionally damped ECM provides the catalyst for the ion-acoustic instability.

In the lower part of the E-region (about 90–100 km) the collision frequencies are given by (Huba 1994)

$$\nu_{in} \approx 2 \times 10^3 \text{ s}^{-1}, \quad \nu_{en} \approx 1.5 \times 10^4 \text{ s}^{-1}, \tag{3.5a}$$

and the gyrofrequencies are

$$\Omega_i \approx 2 \times 10^2 \text{ rad s}^{-1}, \qquad \Omega_e \approx 6 \times 10^6 \text{ rad s}^{-1} \tag{3.5b}$$

where we have used singly charged O_2^+ ions and $B_0 = 0.35$ G, appropriate to the lower ionosphere at equatorial latitudes. Since $\nu_{in}/\Omega_i \approx 10$ (the ions are approximately unmagnetized) and $\Omega_e/\nu_{en} \approx 4 \times 10^2$, we see that the quantity ψ, given by (3.3b), and written in the form

$$\psi = \frac{\Omega_e \nu_{in}}{\nu_{en} \Omega_i} \left[1 - \frac{\sin^2 \theta}{1 + (\nu_e/\Omega_e)^2} \right], \tag{3.6}$$

goes from a large number $\approx 4 \times 10^3$ at $\theta = 0$ to a small number $\nu_{en}\nu_i/\Omega_e\Omega_i \approx 1/40$ at $\theta = \pi/2$. Hence the instability condition (3.4), namely,

$$M_\perp \sin\theta > (1 + \psi), \tag{3.7}$$

states that only those waves propagating nearly along the x-axis ($\theta = \pi/2$) can be driven unstable for Mach numbers $M_\perp (U_e/c_{ei})$ moderately in excess of unity. For example, with $E = 10$ mV m^{-1} and $B = 10^4$ nT, the convection speed U is 1 km s^{-1}, whereas the ion-acoustic speed is about 1/3 km s^{-1} (based on $T_e = 10^3$ K and O_2^+ ion mass). Hence it is sufficient to replace θ by $\pi/2$ in (3.6) and (3.7) which become

$$\psi \approx \frac{\nu_{en}\nu_{in}}{\Omega_e \Omega_i} \ll 1 \tag{3.8a}$$

and

$$M_\perp \gtrsim 1. \tag{3.8b}$$

The corresponding growth rate approximates to

$$\gamma = \frac{\nu_{in}}{\Omega_e \Omega_i} (c_{ei}^2 k^2)(M_\perp^2 - 1). \tag{3.8c}$$

In a recent paper, Buchert et al. (2006) invoked this FB instability as the source of plasma density irregularities in the auroral and equatorial electrojets and considered the effects of such a spectrum of (neutrally stable) turbulent modes on the DC currents giving rise to the irregularities.

The effects of ion plasma frequency (space charge effects) on the frequency and threshold condition are rather small for wavelengths greater than the Debye length. To zeroth order we obtain formulae (3.3a) and (3.3c) in which ψ is replaced by $\psi/(1 - \omega_r^2/\omega_p^2)$, with the threshold condition being modified to

$$(\mathbf{k} \cdot \mathbf{U}_e)^2 > \frac{c_{ei}^2 k^2}{(1 - c_{ei}^2 k^2)/\omega_{pi}^2} \left(i + \frac{\psi}{(1 - \omega_r^2/\omega_{pi}^2)} \right), \tag{3.9a}$$

https://doi.org/10.1017/S002237780600612X Published online by Cambridge University Press

with the corresponding growth rate

$$\gamma = \frac{\psi}{\nu_{\rm in}(1-\omega_{\rm p}^2/\omega_{\rm pi}^2)}\left[\omega_{\rm r}^2\left(1+\frac{c_{\rm ei}^2k^2}{\omega_{\rm pi}^2}\right)-c_{\rm ei}^2k^2\right]. \tag{3.9b}$$

4. High-frequency instability: resonance between electron-cyclotron and ion-acoustic modes

There is another instability embedded in the general dispersion relation (2.19), which emerges most clearly from the collisionless case ($\nu_{\rm e} = \nu_{\rm i} = 0$), in which electron inertia is retained. The dispersion equation may be written as

$$(\omega^2-\omega_{\rm a}^2)(\omega_{\rm e}^2-\omega_{\rm ec}^2) = \frac{m_{\rm e}}{m_{\rm i}}(\Omega_{\rm e}^2-\omega_{\rm e}^2)\omega_{\rm e}^2\left(1-\frac{\omega^2}{\omega_{\rm pi}^2}\right), \tag{4.1a}$$

where

$$\omega_{\rm a}^2 \equiv c_{\rm ei}^2k^2\left(1-\frac{\omega^2}{\omega_{\rm pi}^2}\right), \quad \omega_{\rm ec}^2 \equiv \Omega_{\rm e}^2\cos^2\theta, \quad \omega_{\rm e} = \omega - \mathbf{k}\cdot\mathbf{U}_{\rm e}, \tag{4.1b}$$

in which we have assumed cold ions ($c_{\rm i} = 0$) and neglected their streaming, $U_{{\rm i}y} = 0$. In this form the ion-acoustic mode $\omega^2 = \omega_{\rm a}^2$ (a sphere in $\mathbf{k}$-space) is coupled to the electron-cyclotron mode $\omega_{\rm e}^2 = \omega_{\rm ei}^2$ (a cone in $\mathbf{k}$-space distorted by the electron streaming) by the term on the right-hand side of (4.1a). Therefore, we should expect instability if the frequency of a backward propagating ECM, blown forward along the x-axis by the electron streaming (E_0/B_0 drift), $\omega_{\rm e} = -\omega_{\rm ec}$ matches that of a forward propagating ion-acoustic mode, $\omega = \omega_{\rm a}$, as indicated in Fig. 2, in which the intersection between the distorted cone and sphere are indicated by O. By letting

$$\omega - \omega_{\rm a} = -i\gamma \quad \text{and} \quad \omega_{\rm e} + \omega_{\rm ec} = -i\gamma, \tag{4.2a}$$

(4.1a) yields the growth rate γ as

$$\gamma = \frac{\sqrt{\Omega_{\rm e}\Omega_{\rm i}}}{2}\sin\theta\sqrt{1-\frac{\omega_{\rm a}^2}{\omega_{\rm pi}^2}}. \tag{4.2b}$$

This type of instability is structurally similar to those which arise in electrostatic parametric resonances (McKenzie and Hagfors 1996), or in multi-ion plasmas (McKenzie et al. 1993). In the latter case there exists differential streaming between the ions, as is the case of alpha particles and protons in the solar wind. In these cases a 'negative' energy wave interacts with a 'positive' energy wave in the presence of background steaming to give rise to instability. Cairns (1979) has also discussed the role of negative energy waves in some instabilities of parallel flows. In the case at hand, the 'negative' energy wave is the backward propagating ECM, $\omega_{\rm e} = -\omega_{\rm ec}$, convected forward by electrons streaming with the drift speed E_0/B_0 along the x-direction, and this wave couples to the 'positive' energy ion-acoustic mode, at the unstable points marked ∘ in Fig. 2. However, in the presence of collisions with neutrals there exists a threshold which may be calculated from the dispersion

https://doi.org/10.1017/S002237780600612X Published online by Cambridge University Press

equation, which now approximates to

$$\left(\omega-\omega_{\rm a}-\frac{i\nu_{\rm in}}{2}\right)\left(\omega+\omega_{\rm a}-\frac{i\nu_{\rm in}}{2}\right)(\omega_{\rm e}-i\nu_{\rm en}+\omega_{\rm ec})(\omega_{\rm e}-i\nu_{\rm en}-\omega_{\rm ec})$$

$$=\frac{m_{\rm e}}{m_{\rm i}}\omega_{\rm e}(\omega_{\rm e}-i\nu_{\rm en})[\Omega_{\rm e}^2-(\omega_{\rm e}-i\nu_{\rm en})^2]\left(1-\frac{\omega_{\rm a}^2}{\omega_{\rm pi}^2}\right). \tag{4.3a}$$

Substituting (4.2a) into (4.3a) yields the equation for the growth rate γ, namely,

$$\left(\gamma+\frac{\nu_{\rm i}}{2}\right)(\gamma+\nu_{\rm e})=\frac{\Omega_{\rm e}\Omega_{\rm i}}{4}\sin^2\theta\left(1-\frac{\omega_{\rm a}^2}{\omega_{\rm pi}^2}\right). \tag{4.3b}$$

Hence instability ($\gamma>0$) requires

$$\left(1-\frac{\omega_{\rm a}^2}{\omega_{\rm pi}^2}\right)\Omega_{\rm e}\Omega_{\rm i}\sin^2\theta>2\nu_{\rm in}\nu_{\rm en}, \tag{4.3c}$$

since the growth rate is now given by

$$\gamma=\frac{1}{2}\left\{\left[\left(\frac{\nu_{\rm i}}{2}+\nu_{\rm e}\right)^2+\left[\Omega_{\rm e}\Omega_{\rm i}\sin^2\theta\left(1-\frac{\omega_{\rm a}^2}{\omega_{\rm pi}^2}\right)-2\nu_{\rm i}\nu_{\rm en}\right]\right]^{1/2}-\left(\frac{\nu_{\rm i}}{2}+\nu_{\rm i}\right)\right\}. \tag{4.3d}$$

The resonance condition,

$$\omega_{\rm a}=-\omega_{\rm ec}, \tag{4.4a}$$

as depicted in Fig. 2, yields the obliqueness of the wave normal of the unstable waves and simply requires $M_{\rm c}>1$ to yield the intersections marked $\circ$ in Fig. 2.

The angle $\theta_{\rm r}$ of the (possibly) unstable waves follows from the resonance condition (4.4a) which gives the intersections of the acoustic circle, namely,

$$k_\parallel^2+k_\perp^2=\frac{1}{(1-\omega^2/\omega_{\rm pi}^2)}\equiv r_{\rm a}^2, \tag{4.4b}$$

with the Doppler shifted electron-cyclotron cone,

$$k_\parallel^2=\frac{k_\perp^2(1-k_\perp M_\perp)^2}{[\overline{\omega}^{-2}-(1-k_\perp M_\perp)^2]}, \tag{4.4c}$$

in which $\mathbf{k}$ is normalized to $\omega/c_{\rm ei}$, $\overline{\omega}=\omega/\Omega_{\rm e}$ and $M_\perp=U_{\rm e}/c_{\rm ei}$. Hence $\theta_{\rm r}$ is given by

$$\cos(\theta)=\frac{k_\perp}{r_{\rm a}}=\overline{\omega}^2 r_{\rm a}\frac{[M_\perp+(\overline{\omega}^2 r_{\rm a})^{-1}\sqrt{1+\overline{\omega}^2(r_{\rm a}^2M_\perp^2-1)}]}{1+\overline{\omega}^2(r_{\rm a}^2M_\perp^2)}. \tag{4.4d}$$

Substituting this value for θ_r into the threshold condition yields the frequency bands of the instability and the Mach number $M_\perp$ of the electron streaming required to drive the instability.

Since the quantity $2\nu_{\rm in}\nu_{\rm en}/\Omega_{\rm e}\Omega_{\rm i}$ is small, about 1/10, in the lower E-region, it would at first sight appear that almost all waves, other than those parallel to $\mathbf{B}_0$ ($\theta_{\rm r}=0$), would be excited with growth rates of the order of $\sqrt{\Omega_{\rm e}\Omega_{\rm i}}/2\sim 2\times10^4\ {\rm s}^{-1}$. However, a closer examination of (4.4d) for the resonant angle $\theta_{\rm r}$ shows, in fact, that the resonant angle θ_r is extremely small, with

$$\sin^2\theta_{\rm r}\approx\overline{\omega}^2(M_\perp^2-2M_\perp), \tag{4.4e}$$

https://doi.org/10.1017/S002237780600612X Published online by Cambridge University Press

since $\overline{\omega} = \omega/\Omega_e$ has an upper limit of ω_{pi}/Ω_e, which is $O(10^{-2})$ in the E-region. If the space charge effects are included, through r_a, then

$$\cos(\theta_r) \approx \frac{\sqrt{1-\omega^2/\omega_{pi}^2}}{\overline{\omega} M_\perp}, \tag{4.4f}$$

which shows that a narrow band of frequencies, just less than the ion plasma frequency, are excited with θ_r going from $\pi/2$ (at $\omega = \omega_{pi}$) to 0 (at $\omega = \omega_{pi}/\sqrt{1+M_\perp^2\omega_{pi}^2/\Omega_e^2}$).

The threshold condition (4.3c) now becomes

$$L \equiv \left(1-\frac{\omega^2}{\omega_{pi}^2}\right)\left[1-\frac{1}{\overline{\omega}^2 M^2}\left(1-\frac{\omega^2}{\omega_{pi}^2}\right)\right] > \frac{2\nu_{in}\nu_{en}}{\Omega_e\Omega_i}. \tag{4.5a}$$

The maximum value of the left-hand side, L, occurs at

$$\frac{\omega}{\omega_{pi}} = \left(1+\frac{\omega_{pi}^2 M_\perp^2}{\Omega_e^2}\right)^{-1/4}, \tag{4.5b}$$

with $L_{max} \approx \omega_{pi}^2 M_\perp^2/2\Omega_e^2$. Hence the threshold Mach number is

$$M_\perp > 2\sqrt{\frac{\nu_{in}}{\Omega_i}\left(\frac{\nu_{en}\Omega_e}{\omega_{pi}^2}\right)} \equiv M_c. \tag{4.5c}$$

In the lower E-region M_c is about 20, which implies that very strong electric fields of the order of 75–100 mV m^{-1} are required to drive the instability. However, in the middle to upper E-region, on the day-side where ω_{pi} is around 10^5 rad s^{-1}, the collision frequencies have decreased by an order of magnitude ($\nu_{in} \approx 10^2$ s^{-1}, $\nu_{en} \approx 9 \times 10^2$ s^{-1}) with the result that the critical Mach number M_c drops to around unity, which implies that electric fields, of the order of 5 mV m^{-1} (roughly the order of magnitude of vertical electric fields in disturbed conditions in the equatorial electrojet), can drive this instability. The characteristic growth rate, given by (4.2b), is of $O(\sqrt{\Omega_e\Omega_i}/2)$ which is around 2×10^4 s^{-1}, but is modified by collisions according to the above discussion, and shows that a narrow band of frequencies, just less than the ion plasma frequency, are excited over a wide range of angles, except those very close to $\theta_r = 0$ and $\theta_r = \pi/2$.

5. Summary and conclusions

This paper generalizes the classical FB instability to include space-charge effects and electron inertia, with the latter giving rise to the propagating ECM weakly damped by collisions with neutrals for wave frequencies greater than the collision frequency and less than the electron gyrofrequency. In the presence of electron streaming, the wave normal surface of this mode is distorted from its conical surface by Doppler shifting and resembles a cone squashed between two planes, as depicted in Fig. 1. Of particular interest here is the branch in the figure which lies between $k_\perp = 1/M_\perp$ and $k_\perp = (1+\overline{\omega}^{-1})/M_\perp$ since the wave frequency of this branch, as observed in the rest frame, is negative and the wave may be thought of as carrying negative energy. The interaction between this mode and the forward propagating ion acoustic mode, as interpreted graphically in Fig. 2, gives rise to a new instability whose growth rate is around one half of the lower hybrid frequency

https://doi.org/10.1017/S002237780600612X Published online by Cambridge University Press

(4.2b) somewhat modified by collisions and the resonant wave normal angle θ_r. For conditions prevailing in the middle, day-side, E-region the instability requires $M_\perp > M_c \approx 1$ and generates a narrow spectrum of waves just below the ion plasma frequency. Therefore, the role of this instability in electrojet dynamics and irregularities warrants further careful appraisal and study.

Acknowledgements

The author thanks Professors T. Hagfors and T. B. Doyle for fruitful discussions. The work was carried out at the University of California, Riverside and the University of KwaZulu-Natal, with the support from the National Research Foundation of South Africa (grant number 2053776) and a NASA grant NNGO4GF83G and NSF grants ATM031509 and ATM04288880.

References

Buchert, S. C., Hagfors, T. and McKenzie, J. F. 2006 Effects of electrojet irregularities on DC current flow. *J. Geophys. Res.* **111**, A02305, doi:10.1029/2004/JA010788.

Cairns, R. A. 1979 The role of negative energy waves in some instabilities of parallel flows. *Fluid Mech.* **92**, 1–14.

Fejer, B. G., Providaki, J. and Farley, D. T. 1984 Theory of plasma waves in Auroral E-region. *J. Geophys. Res.* **89**(A9), 7487–7494.

Hamza, A. M. and St.-Maurice, J.-P. 1993 A turbulent theoretical framework for the study of current-driven E region irregularities at high altitudes: basic derivation and application to gradient-free situations. *J. Geophys. Res.* **12**, 40–43.

Huba, J. D. 1994 NRL Plasma Formulary. NRL/PU/6790-94-265, Naval Research Laboratory, Washington, DC, p. 42.

Janhunen, P. 1995 On recent developments in E-region irregularity simulations and a summary of related theory. *Ann. Geophys.* **13**, 791–806.

Liperovsky, V. A., Meister, C.-V. and Kustov, A. V. 2006 Stabilization of the Farley–Buneman instability by three waves interaction as consequence of the modification of the speed of energy transfer from an electric field. *Astron. Nachr.* **320**(2), 77–85.

McKenzie, J. F. and Hagfors, T. 1996 Electrostatic parametric resonances in a plasma, revisited. *J. Plasma Phys.* **55**(3), 359–385.

McKenzie, J. F., Marsch, E., Baumgärtel, K. and Sauer, K. 1993 Wave and stability properties of multi-ion plasmas with applications to winds and flows. *Ann. Geophys.* **11**, 341–353.

Milikh, G. M. and Dimant, Y. S. 2003 Model of anomalous electron heating in the E region: 2 Detailed numerical modeling. *J. Geophys. Res.* **108**(A9), 1351, doi:10.1029/2002/JA009527.

Oppenheim, M., Otani, N. and Ronchi, C. 1996 Saturation of the Farley–Buneman instability via nonlinear electron $E \times B$ drifts. *J. Geophys. Res.* **101**, 17 273–17 286.

Robinson, T. R. 1994 The role of E-region plasma turbulence in the enhanced absorption of hf radio waves in the auroral ionosphere: implications for RF heating of the auroral electrojet. *Ann. Geophys.* **12**, 316–332.

Robinson, T. R. 1998 The effects of small scale field aligned irregularities on E-region conductivities: implications for electron thermal processes. *Adv. Space Res.* **22**, 1357–1360.

Sudan, R. N. 1983 Nonlinear theory of type I irregularities in the equitorial electrojet. *J. Geophys. Res.* **88**, 40.

Weinstock, J. and Sleeper, A. 1972 Nonlinear saturation of type I irregularities in the equitorial electrojet. *J. Geophys. Res.* **77**, 3621–3629.

https://doi.org/10.1017/S002237780600612X Published online by Cambridge University Press